INTERNATIONAL JOURNAL OF
COASTAL & OFFSHORE ENGINEERING IJCOE Vol.5/No. 1/Spring 2020 (31-43)

Available online at www. ijcoe.org

# Seismic Design of Subsea Jumper per ISO:

## Part I- Preliminaries

**Sirous F. Yasseri**

*Brunel University London; Sirous.Yasseri@Brunel.ac.uk;*

**ARTICLE INFO**

*Article History:*
Received: 28 Aug. 2020
Accepted: 14 Nov. 2020

*Keywords:*
Subsea Spools
Soil- spool interaction
ISO 19901
ISO 19902
Geohazard
ALE and ELE

**ABSTRACT**

Subsea rigid steel spools (spool) are used to connect subsea equipment using diver-less connectors. Spools must meet functional requirements such as pressure, temperature, thermal expansion, environmental load, installation loads, lack of fit (misalignments), etc., yielding numerous loading conditions. The installation accuracy that the installation contractor can achieve is another issue. Thus, it is inevitable that numerous geometries to be investigated and perform several iterations in search of a suitable configuration. The no-burst concept, in conjunction with a High Integrity Pressure Protection (HIPP) system, leads to heavier spool wall thickness, hence less structural flexibility which in turn increases reactions on the subsea connectors, which in turn is transferred to the adjoining equipment. Add to this complexity, the seismic qualification requirement if a jumper is in an earthquake-prone area.

This is the first part of a three-part paper that discusses experiences gained in designing spools in 500m of water. The primary focus of the paper is on seismic design, but other issues are discussed including loading & load combinations, increasing the structural flexibility without lowering the natural frequencies; limitation imposed by the subsea connectors, the neighboring equipment loads, and tolerances. Generally, the capacity envelope of connectors will govern most of the time.

These papers build on the existing literature and liberally draws from them. The objective is to summarise and bring together existing research data needed to design subsea rigid spools.

## 1. Introduction

Deepwater pipelines are connected to manifolds/trees/FTA/ITA by utilizing diver-less mechanical connectors and rigid spools. Deepwater rigid spools must accommodate expansion displacement due to high product temperatures, possible soil's low strength, and other phenomena such as pipe walking and debris flows. Spools must also accommodate fabrication and installation tolerances. These requirements, and others, derive the spool geometry and can lead to complex configurations that cause installation difficulties.

An issue requiring investigation is the selection of vertical or horizontal orientation of the connection system (Figure 1). The geometry of the field and installation vessel may also be determining factors. Each orientation exhibits several advantages and disadvantages. However, both systems have been proven as an acceptable solution

There are 2 main types of connectors used in deep-water applications. Figure 2 shows typical horizontal and vertical connectors as well as one type of flanged connections.

The structure of these three interlinked papers are as follows:

Part 1: deal with the background data

Part 2: Describes ISO requirements and derivation of earthquake time histories

Part3: Describe the design of subsea spools with a focus on the seismic design.

**(a): Horizontal Spool**

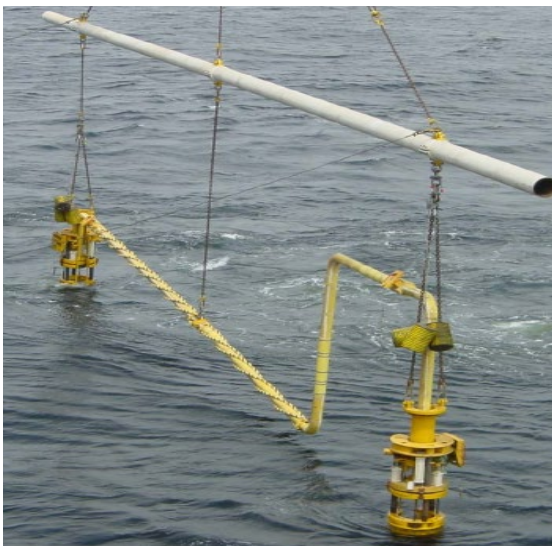

**(b): Vertical Spool**

**(c): a complex Spool**

**Figure 1. Three types of geometry (courtesy of JP Kenny)**

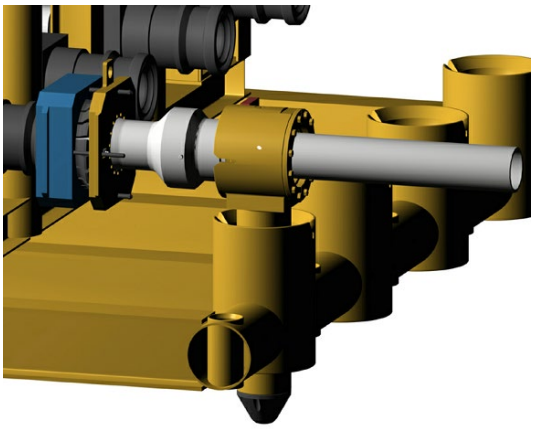

**(a): Horizontal Connector**

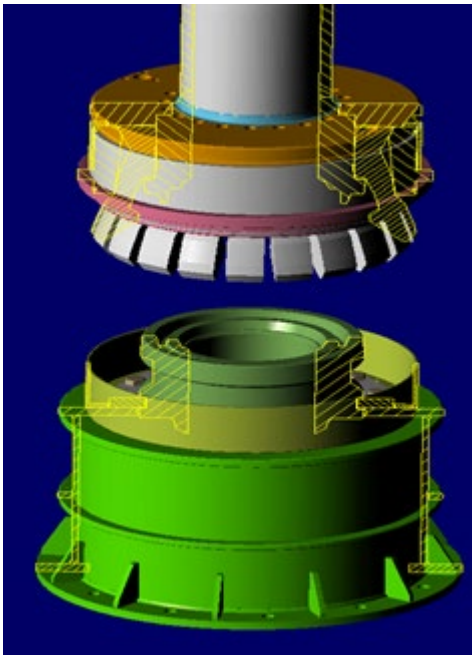

**(b): Vertical Connector**

**( C) Typical flanged connection (diver assisted)**

**Figure 2. Typical Horizontal and Vertical Connectors (courtesy of JP Kenny)**

Typical connector loads (Bending Moment) could be approaching the limits of the pipe on the spool piece assembly. The connector supplier needs to be aware of this and shall be able to offer a suitable pup-piece design (e.g. forged) as required. Connector loading capacity shall be confirmed by the connector supplier during Request for the information by spool designers. Figure 3 shows spools with a very complex geometry if a rigid spool is used.

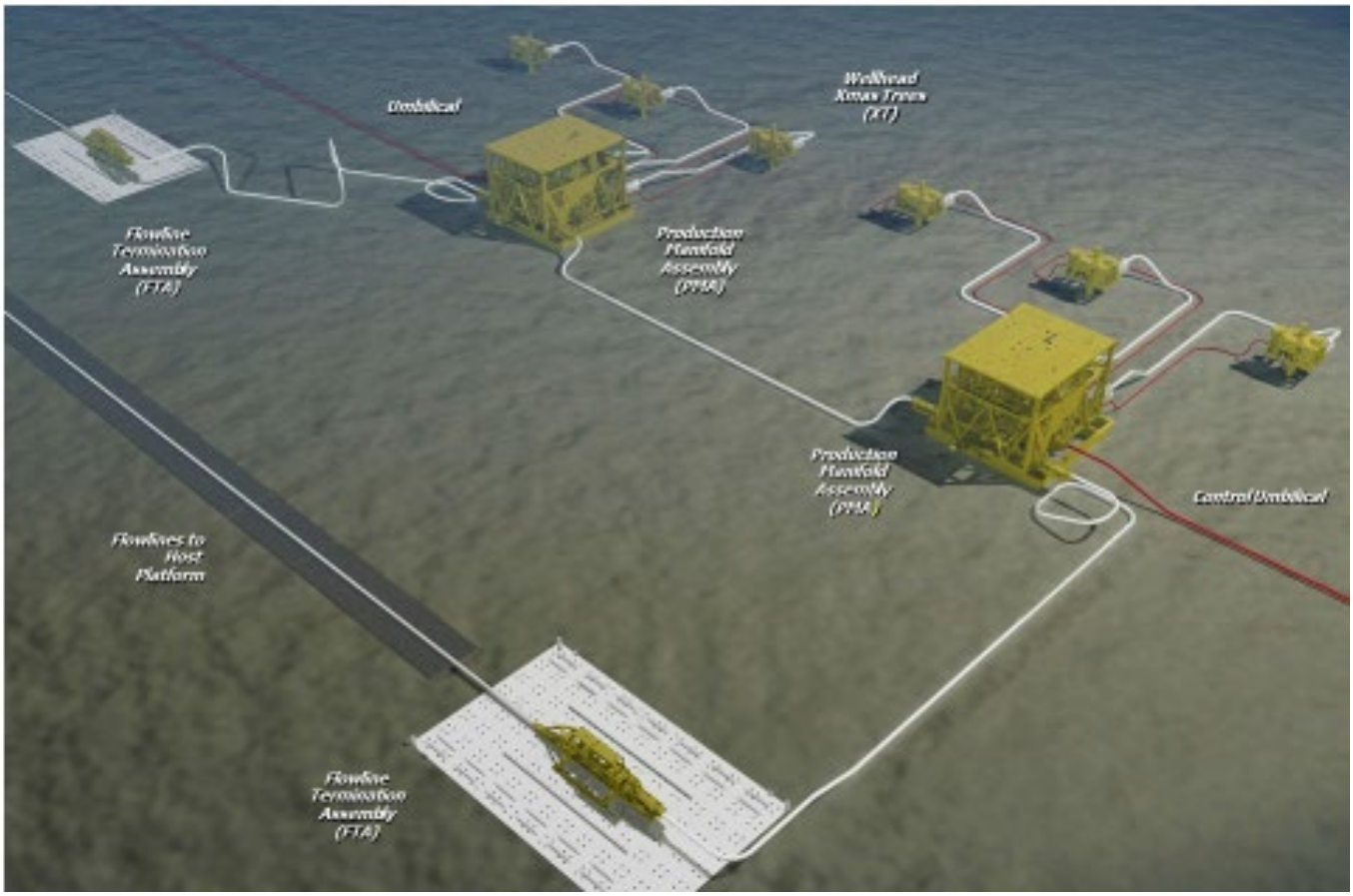


**Figure 3. A cluster-type subsea architecture consisting of two manifold each connected to three X-trees.**

Most often than not, deep-water spools are stretched to fit into the subsea connectors' receptacles, which creates substantial stresses in a thick-walled rigid spool. Operational loads (pressure and temperature), installation tolerances, and lack of fit aggravate this situation. High pressure requires heavier wall thickness which reduces the much-needed flexibility. If the region happens to be moderately seismically active, then the design is more demanding. In general, the capacity of a jumper is almost exhausted before the application of the seismic load. Adding more flexibility would alleviate his problem but could create another problem, which is making the spool prone to flow-induced vibrations. Thus, obtaining an optimal solution requires a lot of searching in the solution space. Though dealing with seismic load is the focus of this paper, other loads that a spool is expected to withstand must be borne in mind since their severity determines how much margin is left for the seismic loading. There are cases where using a rigid spool is almost impossible and flexible pipes are used instead.

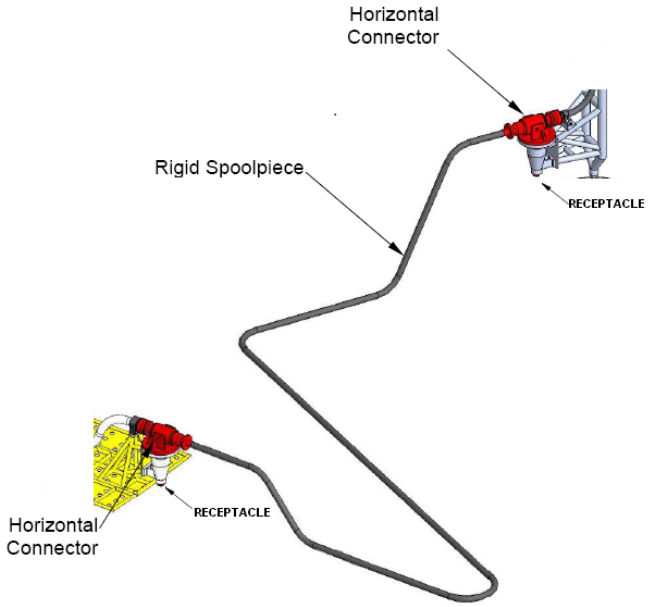


**Figure 4. Once the subsea structures have been installed the distance between the connectors and the angular alignment of the hubs will be established by the survey.**

## 2. Tolerances

Spool pieces are designed to accommodate installation errors, which put a heavy demand on them. However, there is a limit to what can be achieved, hence some tolerances must be imposed on all possible errors (Figure 4).

Tolerances that need to be considered are:

• Structure Installation Tolerances

• Metrology & Fabrication (tolerance between metrology reference e.g. stab receptacle on the lower structure, and inboard hub)

• Connector system tolerances

• Installation Tolerances

### 2.1. Tolerance for the structure (Typical installation

Based on the industry practice tolerances for wellhead guide bases, manifolds, Flowline termination assembly, and in-line tees are given below:

Wellhead Guide-bases: Verticality ± 2 deg

Azimuth ± 15 deg

Manifolds Verticality ± 3 deg

Azimuth ± 5 deg

FTAs/in-line tees Verticality ± 5 deg

Distance between pairs of Christmas tree (x-tree) connection tie-in points:

25 ± 10 meters

Distance between production manifold and flowline connection:

35 ± 5 meters

The spool configuration must possess adequate length, and angular capacity to accommodate these tolerances. If pre-fabricated spool elements are used they must have sufficient green material for cutting to size.

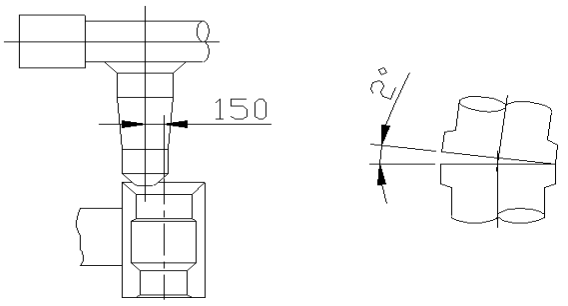


**Figure 5. Connector's system Tolerances (courtesy of JP Kenney)**

### 2.2. Metrology and Fabrication Tolerances

Once the subsea structures have been installed the distance between the connectors and the angular alignment of the hubs will be established by the survey (Figure 5).

These sizes are used to fabricate the spools to fit.

Typical metrology and fabrication tolerances are:

± 150mm in any three axes

± 2 degrees in any three axes

### 2.3. Connector's system Tolerances

Hub to connector tolerances arises from several sources including fabrication tolerances for the inboard structures, stack-up tolerances for two-part structures, and also the requirement that production spool shall be re-usable after tree interventions.

These followings are considered in the stress analyses of spools.

- Combinations of Extreme Tolerance and Misalignments

The angular & linear tolerances due to metrology & spool fabrication and misalignments could all be forced on the spool system during the installation and stroking connection. The spool shall be designed to accommodate all the possible combinations of angular & linear tolerances and misalignments.

- Connector Stroking ( Figure 6)

Stroking length shall be considered in the stress analysis; it should be noted that where possible the local architecture has been adjusted so that stroking reduces maximum stresses.

### 2.4. Installation Tolerances

A distinction should be made between the installation tolerances, which will be quantified during offshore metrology, and the other 'residual' tolerances

The offshore installation tolerance shall be accommodated within the design of prefabricated spool kits that will have angular and length adjustment on 'closing' welds during spool fabrication.

The other tolerances shall be accommodated in the design flexibility of the spools.

The angular & linear tolerances due to metrology & spool fabrication and misalignments could all be forced on the spool system during the installation and stroking connection. The spool shall be designed to accommodate all the possible combinations of angular & linear tolerances and misalignments.

Metrology and spool fabrication have their tolerances which could cause misalignment at the connector hub face. Consequently, additional loads could arise from spool deformation because of induced forces during installation to match-up the connector faces.

The magnitude of these additional loads is dependent on the stiffness of the system near the connectors.

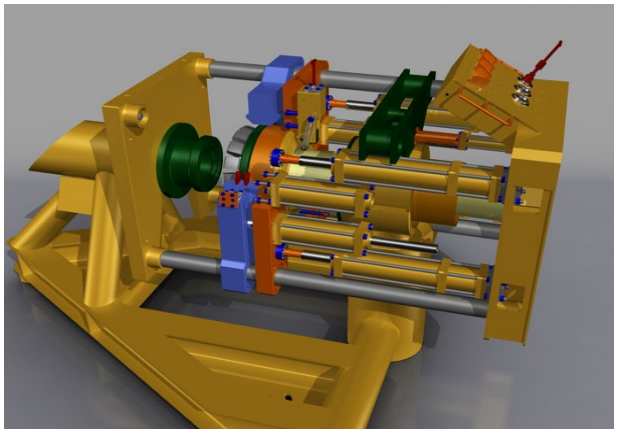

**(a): Before stroking**

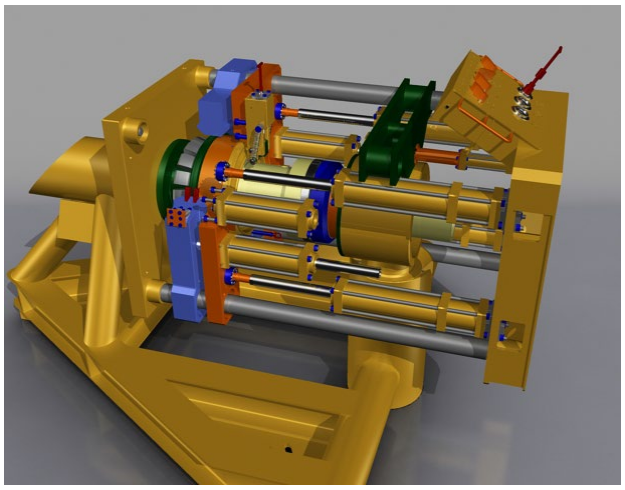

**(b): After Stroking**

**Figure 6. Connectors' stroking**

The following are a few consideration to mitigate the loading:

- The stiffness of the path through which the load travels from the connector into the inboard hub to the mounting structure as well as the steelwork of the inboard structures must be considered, which would allow for flexibility, hence reduction in connector loads
- Modeling the misalignments tolerances with kinematics constraints, this would provide certain flexibilities within the system, hence lower the localized bending moments at the connector supporting system.

## 3. Spool Installation Issues

A reasonable installation assessment that should be considered during the engineering design should be based on the following criteria:

• Installation is feasible with appropriate engineering input on 60-meter accumulative length (the pipe length) and 45-meter envelope (distance between connector to connector).

• Spool installation complexity and increased risks are introduced when the spool length is the 70-meter accumulative length and 50-meter distance between connector to connector.

• the spool width must be kept to the minimum.

• The center of gravity of the spool should be kept close to the main axis of the spool.

• The center of gravity, weight, geometry, flexibility, and the torsional stiffness of the spools are such that the complexity size and weight of the spreader bar and rigging are minimized.

• The lift capacity of the vessel crane at the required offset should be adequate.

• The lift capacity of the vessel crane is adequate given the crane radius and the appropriate dynamic amplification factor, skew loads, weight, and center of gravity of the spool uncertainty factors.

•For installation of rigid spools commonly they are lifted off the deck of the installation vessel or barge/supply vessel and lowered using the vessel's crane and either directly installed or abandoned and recovered by the winch.

## 4. Spool -soil interaction

When a spool that is resting on the seabed is subjected to transient loads, it interacts with the soil such that a continuous transfer of energy takes place between them. The effect of interaction on the dynamic behavior of a Spool is determined by the mechanical properties of spool and soil and the interaction mechanism and the type of dynamic loading (Ghannad et al [14], Ghannad et al [15], and Jafarieh and Ghannad [17]). The kind and intensity of the interaction depend on the physical processes that occur at the interfaces between them (see e.g. Gazetas and Dobry [ 11 and 12] and Gazetas [9 and 10]).

Analysis of spool–soil interaction for the design purpose requires a simplified, but a conservative, method, since it is not practical to model the entire soil-spool systems, to be modeled in great detail. The size of the overall system is so large that it's exact modeling by finite element methods is computationally expensive. Engineers are mainly interested in the response of the spool, and the soil to the extent it affects the spool, thus accurate modeling is only needed for the spool. Therefore, the overall system can be subdivided into subsystems with a suitable interface and imposed boundaries.

The far-field is not bounded and thus has an important effect on the wave dynamics. Waves that re traveling in the unbounded direction, cannot reflect as there are no hard boundaries. Because waves transport energy and in a real situation they won't return, we obtain a mechanism which irreversibly transfers energy from the near field to the far-field. This mechanism is called radiation damping which extracts energy from the near field (Lysmer & Kuhlmeyer, [16]). The effect is not dissimilar to that of viscous damping where some of the

energy is irreversibly converted into heat. The response of the structure will be very much reduced. For this kind of problem, the accurate modeling of radiation damping becomes a central issue (El Naggar & Bentley [5]). This is exactly the case for spools interacting with the seabed.

The method of implementing this radiation damping is also an issue. For practical reasons, the finite element model must be of a reasonable size. One approach is to model a finite portion of the soil using solid elements with defined soil behavior and properties. Then layers of elements are added around this model and allow them to absorb energy. This boundary layer is known as the silent boundary, the quiet boundary, the absorbing boundary, or transmitting boundaries. Most software packages have implemented the Lysmer & Kuhlmeyer [16] formulation. The element type is known as the infinite element with viscous damping capability. Abaqus element library includes such elements. Infinite elements take care of both far-field displacement and non-reflective boundary. An approximation would be to attach dashpots and springs to the model boundary to model the far-field stiffness and prevent reflection of the wave at the boundary. There are other variations of representing the far-field effect.

In addition to the radiation damping, internal friction in the soil also dissipates the seismic energy (Hardin & Drnevich[13]). In all cases, the soil material damping is assigned in the material definition, as the soil is explicitly represented in this type of modeling.

Given the number of cases to run for the design of spools, the above approach is only practical for the confirmatory final run. For design purposes, a simplified approach is used which is known as a beam on the Winkler foundation, where a spool is assumed to rest on a bed of springs (linear or no-linear). This simple approach gives very good results for the spools which is the focus of the attention here while providing no information for the soil strains and displacement. There is a variety of ways to implement the idea of Bean on Non-linear Winkler Foundation (BNWF); see for example Vesic [32], El Naggar [6], El Naggar et al [7], or Boulanger et al [4].

Beams on the nonlinear Winkler foundation (BNWF) method has been used extensively to model the soil-pipe interaction when both inelastic behavior and dynamic effects are present. BNWF models can account for various complex conditions. Among others, Matlock et al.[24], Novak [26], Nogami et al [25], Makris and Gazetas [23], and El Naggar and Bentley [5] used BNWF models for piles subjected to lateral dynamic loads.

Boulanger et al. [5] developed a BNWF model utilizing springs in series, with dashpots representing radiation damping. El Naggar and Bentley[5] introduced dynamic *p–y* curves for dynamic lateral response analysis of piles. El Naggar et al[7] proposed a new combination of free-field ground motion analysis and BNWF for nonlinear dynamic response analysis of offshore piles. They used commercial software to verify their proposed BNWF model against the published centrifuge test data on seismic response of piles and they reported a very good fit. Some of these models include the effect of gaping between pile and soil.

In the BNWF method, the spool is represented as a series of discrete beam-column elements resting on a series of springs and dashpots representing the nonlinear dynamic behavior of the soil. To determine the kinematic response, the “free-field” ground motion time histories are calculated in a site response analysis. This idea of a non-linear Winkler foundation can easily be implemented in Abaqus, by defining the seabed as a plane surface with defined flexibility in the vertical direction. The lateral and axial non-linear behavior is defined by frictional characteristics seabed allowing the spool to slip when the shearing force at the interface exceeds the capacity.

Spools on a non-linear Winkler foundation are much simpler than pile-soil interaction; since pile encounter various layers of soil, spools are resting only on one layer for its entire length. This simplifies the representation of the soil in the analysis of the spools. The resistance of the seabed to the axial and lateral movements are modeled with friction at the interface of the spool and the seabed, which resembles an elastic-plastic spring. The slope of the elastic section is controlled by defining a break-out (or sliding) displacement, generally about 1mm. The axial and lateral friction is defined as lower and upper bounds. The upper bound is designed to account for resistance to break out due to probable embedment.

Applying damping to such a model poses some difficulties. Since only the spool material is modeled, applying the steel material damping is straightforward. Generally, Rayleigh damping is used in the time domain direct interaction analysis for the implementation of damping. Damping at the interface for the axial and lateral direction is taken care of by the defined friction at the interface. One could use the contact damping facility to address this interface issue. However, determining the damping coefficient is problematic. Damping in the vertical direction depends on the break-out resistance and velocity of the returning pipe impacting the seabed as well as the soil properties to allow its rebound. This damping is ignored in the current work.

Two other sources of damping are soil hysteretic damping and radiation damping, which are major sources of energy dissipation. These can be implemented by dashpots. In some DNV publications, it is implied that soil hysteretic and radiation damping

may be added to the steel damping and apply these composite damping using the Rayleigh method. An "effective damping" can be introduced using some combination of all damping, but the effective damping depends on soil structure dynamic properties.

In a non-linear time-domain analysis Rayleigh approach is used to implement damping (Spears and Jensen [29]). The problem with the Raleigh method is that its parameters are calibrated using natural frequencies of the system in the linear range; as the natural frequencies change due to complex non-linearity in soil-spool iteration, the Rayleigh effect is unknown. While DNV algebraically adds all damping ratio, Wolf [34 and 35] provides an expression for adding various damping using the natural frequencies of various components in the interacting system. This expression is a function of the soil stiffness and the participating mass which are not easily determined. There is no need for Wolf's simplification [35] as it is quite straightforward to use viscous damping for the soil radiation as well as hysteretic damping in the Abaqus analyses. Later sections discuss how to determine the damping coefficients.

## 5. Soil Dynamic Properties

Inputs for seismic analysis of soil-spool include stiffness and material damping of the soil; Makris & Gazetas, [23]. Soil stiffness can be expressed in terms of the shear wave velocity or the shear modulus. Small-strain shear-wave velocity,$V_s$, is directly related to small-strain shear modulus $G_{max}$ by [28]:

$$G_{max} = \rho V_s^2 \qquad (1)$$

where $\rho$ =mass density of soil. The soil's secant shear modulus may be used to represent the average soil stiffness at high to moderate strains. The relationship between$G_{max}$, G, shear strain $\gamma$, and shear stress $\tau$is illustrated in Figure 7. Also illustrated in this figure is the relationship between the stress-strain hysteresis loop for one cycle of loading and the material damping ratio.

the soil's material damping, D is an indicator of the energy dissipation capacity of the soil. The source of material damping is the strain rate effect, friction between soil particles, and nonlinear soil behavior. The hysteretic damping ratio may be determined by

$$D = W_D/(4\pi W_s) \qquad (2)$$

where $W_D$=energy dissipated in one cycle of loading, and $W_s$ =maximum strain energy stored during the cycle. As noted in Figure 7, the area inside the hysteresis loop is $W_D$, and the area of the triangle is $W_S$. Theoretically, there should be no dissipation of energy in the linear elastic range for the hysteretic damping model defined by Equation 2. At relatively low strain levels, energy dissipation is measured using laboratory specimens.

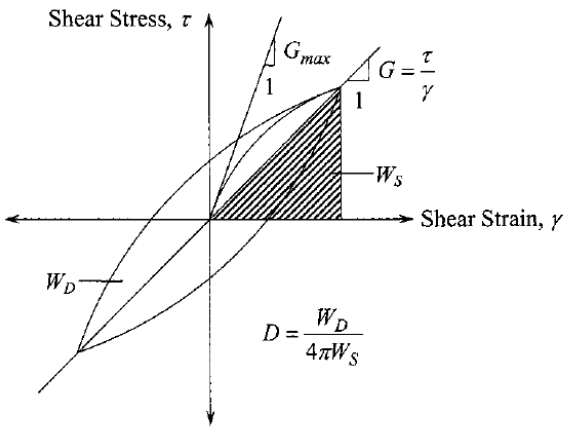


**Figure 7. Hysteretic loo for one cycle of Loading Showing $G_{max}$ , $G$ and $D$**

Note that the damping ratio at very low strain is a constant quantity and is known as the small-strain damping ratio $D_{min}$ . At higher strains, nonlinearity in the stress-strain relationship causes the material damping ratio to increase with increasing strain amplitude.

The current state of practice for determining $G$ and $D$ for ground response analysis involves estimating or measuring$V_s$, in the field and estimating or measuring the variation of $G$ and $D$ with $g$ primarily in the laboratory. It is common practice to normalize $G$ by dividing by $G_{max}$ .

Many studies have been conducted to characterize the factors that influence $G/G_{max}$ and $D$ - See for example; Seed and Idriss [27]; Hardin and Drnevich [13]; Ishibashi and Zhang [22]; Seed et al. [27]; Idriss and Sun et al. [21]; Vucetic and Dobry [33]; Stokoe et al. [30]; Darendeli [31]. This paper primarily uses Idriss and his co-workers' studies.

The most important factors that affect G/Gmax include g, mean effective confining stress, soil type, and plasticity index (PI). Other factors that affect $G/G_{max}$, but appear to be less important, include (according to Darendeli [31]): frequency of loading, number of loading cycles, over-consolidation ratio, void ratio, degree of saturation, and grain characteristics. The most important factors that affect D are g, mean effective stress, soil type, and PI (plasticity Index), frequency of loading, and several loading cycles.

As noted earlier, the dynamic soil properties are defined by the damping ratio and shear modulus degradation curves. These curves were determined for different soil t; e.g. Seed and Idriss [27], and Seed and Sun [21] proposed curves for clay and sand. Seed and Idriss [27] give three curves for the lower bound, the upper bound, and the average values. These curves are shown in Figure 8. The damping curves for sand with the same range of shear strain are shown in Figure 9. Note that lower bound sand refers to less stiff sand with

less damping ratio compared with the upper bound sand at the same shear strain.

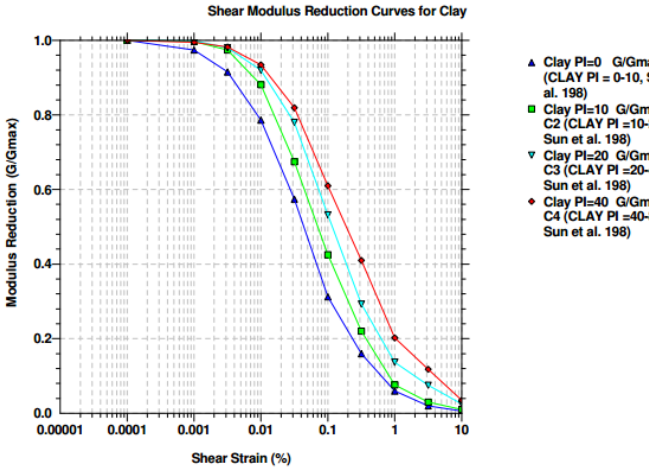


**Figure 8. Shear modulus degradation curve for clay-from [27]**

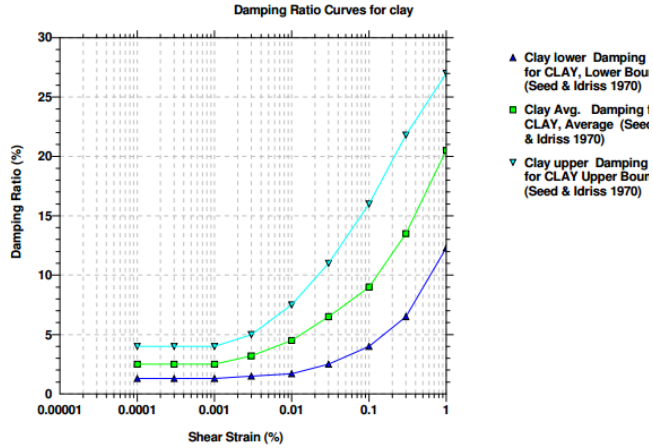


**Figure 9. Damping curves for clay- from [27]**

The shear modulus degradation curves for sand (Figure 9) and the damping ratio curves for san (Figure 10) can be found in Seed and Sun[21]. In the literature, these curves can be found for different levels of the plastic index for clay and different confining pressures for sand.

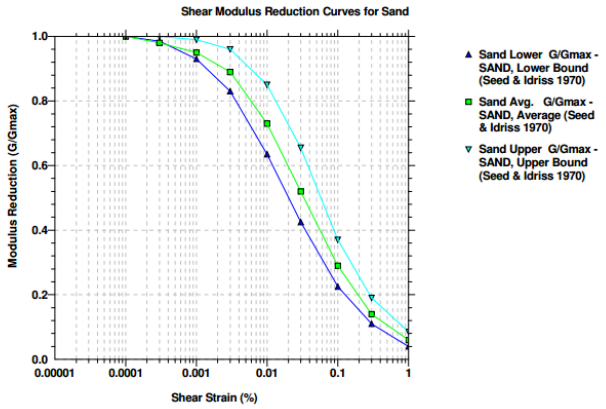


**Figure 10. Shear modulus degradation curve for sand [21]**

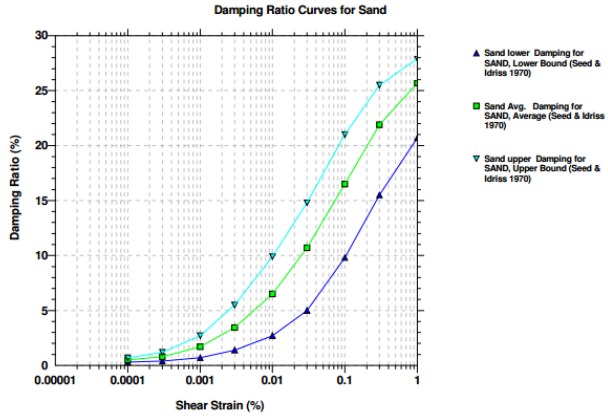


**Figure 11. Damping curves for sand with the same range of shear as in Figure 9 [21]**

## 6. Sources Energy Dissipation

Various frequency-dependent and frequency independent sources of damping that are important for seismic design are:

- Frequency-dependent:
  - Structural material damping
  - Damping resulting locally from strongly nonlinear soil behavior adjacent to the spool
  - Soil material damping of permeable saturated permeable soils (from pore fluid moving relative to the soil skeleton)
  - Energy transport through the soil to the far-field namely the soil Soil radiation damping
  - Hydrodynamic damping, namely the velocity-dependent drag forces acting on the pile
- Frequency independent:
  - Structural friction damping (frictional damping in e.g. bolted connections)
  - Soil material damping for dry and impermeable soils (friction of soil grains moving to each other)

Including all different damping contributions in a mathematical model for earthquake response analysis should conceptually result in the most accurate estimate of the actual response of the structure, but this is quite uncommon in practice. Instead, an equivalent Rayleigh critical viscous damping percentage is often defined to approximate the effects of various damping mechanisms that are present in the real structure. However, the following problems can be named:

- Actual damping resulting from hysteretic behavior often is a nonlinear function of motion amplitude. Consequently, it is not easy to properly include damping in the Rayleigh formulation for dynamic analysis when the motion amplitudes vary strongly.
- By definition Rayleigh viscous damping is frequency-dependent, but the actual damping sources not necessarily are frequency-dependent, for instance,

hysteresis loops due to nonlinearities are frequency independent.

Computational advantages of using linear equivalent viscous Rayleigh damping traditionally were considered to outweigh whatever compromises are necessary for the viscous damping approximation. However, currently, it is believed that in nonlinear dynamic analysis a better approximation of actual damping is obtained when hysteresis behavior (by nonlinearities) and some additional Rayleigh damping are combined. For the low-level responses, the Rayleigh damping portion would govern the total damping, where it becomes negligible compared to the hysteretic energy dissipation for high-level responses.

The sources of damping are explained below:

***Structural material damping-*** Structural damping results from micro-scale material straining (material damping) and friction between surfaces moving relative to each other. The former is related to heat production in materials due to vibrations, which is clearly, depends on the properties. The latter is provided by work done by friction in e.g. connections or other structural slipping surfaces. In practice, material and friction damping of the structure are lumped together into a single equivalent viscous damping parameter. Eurocode 8 [8] recommendations provide an equivalent viscous damping ratio of 5% critical to be included in seismic analysis. ISO 19901-2 and 19902. ISO [18, 19, and 20] recommendations provide maximum modal damping ratios of 5% for fixed steel offshore structures for the ELE events, but additional damping, e.g. hydrodynamic or soil damping, must be substantiated. For fixed steel offshore structures under ALE events where inelastic behavior of both structure and damping is likely, damping values varying up to 10% critical may be applicable. Some codes of practice allow maximum damping values of 5% critical to simulate damping originating from structural joint and hydrodynamic energy dissipation for seismic analysis of fixed concrete offshore structures. Any higher values according to these codes shall be justified by special studies.

***Soil radiation damping:*** Radiation damping is the transport of structural vibration energy to the far-field, and sometimes referred to as geometric damping or attenuation.

***Soil material damping:*** Soil material damping results from frictional forces between soil grains when the soil is vibrating. This friction induces a type of damping that is generally believed to be frequency independent (Hardin and Drenvich [13]) and is characterized by hysteresis soil behavior. For saturated permeable soils, the damping however is characterized better as viscous frequency-dependent damping, since it is governed by pore fluid motion through the soil skeleton generating heat energy. In the past, the soil damping was assumed to be frequency-independent because of convenience. Essentially an equivalent viscosity is defined as $\eta = 2G\zeta/\omega$ resulting in a constant damping ratio. Critical damping percentages can be estimated based on soil shear strain levels, plasticity index, and confining pressure according to Vucetic & Dobry [33]; Ishibashi & Zhang, [22]. In Eurocode 8 [8] an approximation of strain-dependent soil stiffness and damping parameters based on ground accelerations is given. This code allows high-level earthquakes damping ratios exceeding 0.10.

***Damping at the soil-structure interface:*** Increased damping in the soil region surrounding the spool is important. Due to the relatively high deformation levels, extreme hysteresis behavior is locally present, resulting from high local soil strain levels and plastic shearing at the soil-spool interface. Other effects such as scour for clays may contribute to higher damping. The representative damping value strongly dependent on the displacement amplitude. As a consequence of highly plastic local soil behavior adjacent to the spool, radiation damping is reduced by this zone. In this paper, the effect of high strain on the degrading of shear modulus, hence reducing the radiation damping and increasing the soil material damping, is considered by using Idriss's curve (Figures 8 to 11).

***Hydrodynamic damping****:* Spools are surrounded by water. During an earthquake the relative velocities of the pipe and the water are nonzero, drag and inertia forces will result according to Morrison's equation. The drag force varies linearly with the relative velocity of the spool and the surrounding water. Thereby, it forms additional viscous damping. The dependence on the relative velocity of the spool and the water makes the amount of damping difficult to determine during seismic events since the motion of the water itself is an uncertain input parameter. Thus it is uncertain if the hydrodynamic forces damp structure's response continuously or sometimes amplify it. In this paper, the hydrodynamic damping for the earthquake loading is assumed to be zero.

## 7. Soil Radiation Damping for Spools (soil-structure interface)

In dynamic seismic soil-structure interaction, soil damping must be included in the numerical analysis to match numerical and experimental results. However, damping tends to increase for increasing loading rates and frequency. Various researchers (Gazetas & Dobry [12]; Nogami, Otani, Konagai, & Chen, [25]; Makris & Gazetas, [23]; proposed to include a viscous damper parallel to the spring element representing the soil stiffness.

Other researchers (Berger [3], El Naggar [6],; El Naggar & Bentley, [5]) have proposed to define separately the interface, near- and far-field contributions for both linear springs and dashpots.

Both methods have resulted in relatively accurate predictions of dynamic pile response. El Naggar et al [7] compared numerical results with experiments and reported a good fit. The difference between these two approaches is the definition of soil stiffness. Since this stiffness is used to determine the soil damping, hence the amount of damping is different (by about a factor 2). The other difference between them is the first approach includes all six degrees of freedom, while the second method ignores rotational degrees of freedom.

In this work a modified version of the second approach (Berger's approach [3] will be used as described below

ATC-40 [2] has adopted Gazetas formulae. ASCE4-16 [1] uses Lysmer's equation [16] which is a predecessor of Gazeta equations. Eurocode 8 [8] also use a variation of Gazetas formulae for soil-foundation interaction (Table 1).

In this paper, we use a slightly different form for the radiation damping which gives about one-quarter of Gazaetas' values.

**Table 1 Gazetas equations for the shallow foundation as summarised in Applied Technology Council (ATC) (1996). "Seismic Evaluation and Retrofit of Concrete Buildings ATC-40." Volume 1 and 2 November.**

| Stiffness Parameter | Equation |
|---|---|
| | Surface Stiffnesses |
| Vertical Translation | $K_z' = \frac{GL}{1-\nu}\left[0.73+1.54\left(\frac{B}{L}\right)^{0.75}\right]$ |
| Horizontal Translation (toward long side) | $K_y' = \frac{GL}{2-\nu}\left[2+2.5\left(\frac{B}{L}\right)^{0.85}\right]$ |
| Horizontal Translation (toward short side) | $K_x' = \frac{GL}{2-\nu}\left[2+2.5\left(\frac{B}{L}\right)^{0.85}\right]+\frac{GL}{0.75-\nu}\left[0.1\left(1-\frac{B}{L}\right)\right]$ |
| Rotation about x-axis | $K_{\alpha x}' = \frac{G}{1-\nu} I_x^{0.75}\left(\frac{L}{B}\right)^{0.25}\left(2.4+0.5\frac{B}{L}\right)$ |
| Rotation about y-axis | $K_{\alpha y}' = \frac{G}{1-\nu} I_y^{0.75}\left[3\left(\frac{L}{B}\right)^{0.15}\right]$ |
| | Stiffness Embedment Factors |
| Embedment Factor, Vertical Translation | $e_z = \left[1+0.095\frac{D}{B}\left(1+1.3\frac{B}{L}\right)\right]\left[1+0.2\left(\frac{2L+2B}{LB}d\right)^{0.67}\right]$ |
| Embedment Factor, Horizontal Translation (toward long side) | $e_y = \left[1+0.15\left(\frac{2D}{B}\right)^{0.5}\right]\left\{1+0.52\left[\frac{\left(D-\frac{d}{2}\right)16(L+B)d}{BL^2}\right]^{0.4}\right\}$ |
| Embedment Factor, Horizontal Translation (toward short side) | $e_x = \left[1+0.15\left(\frac{2D}{L}\right)^{0.5}\right]\left\{1+0.52\left[\frac{\left(D-\frac{d}{2}\right)16(L+B)d}{LB^2}\right]^{0.4}\right\}$ |
| Embedment Factor, Rotation about x axis | $e_{\alpha x} = 1+2.52\frac{d}{B}\left(1+\frac{2d}{B}\left(\frac{d}{D}\right)^{-0.2}\left(\frac{B}{L}\right)^{0.5}\right)$ |
| Embedment Factor, Rotation about y axis | $e_{\alpha y} = 1+0.92\left(\frac{2d}{L}\right)^{0.60}\left(1.5+\left(\frac{2d}{L}\right)^{1.9}\left(\frac{d}{D}\right)^{-0.60}\right)$ |

Equations to calculate the dashpot constant to account for the soil's energy dissipation are proposed by several researchers. The common practice is to add separate contributions for both hysteretic material damping and radiation damping as:

$$C_{dashpot} = C_r + C_m \quad (3)$$

The material damping is related to the soil's average shear strain amplitude which in turn related to local lateral pile displacement by:

$$\gamma_{avg} = \left(\frac{1+\vartheta}{2.5D}\right) \times (Horizontal\ deformtion\ of\ the\ soil\ layer) \quad (4)$$

The soil horizontal deformation (as a function of depth) is often obtained from simplified dynamic analysis or can be found by an iterative procedure. A damping ratio related to the average shear strain amplitude can be defined, and the dashpot constant then calculated as:

$$c_m = 2k_{secant}\frac{\zeta}{\omega} \quad (5)$$

Berger [3] was among the first to present expressions for the radiation damping. Berger [3] uses the analogy with 1D wave radiation in a rod and accounts for radiation of energy in both the direction of vibration (compression waves) as well as in the transverse direction (shear waves). Berger proposed [3] a dashpot coefficient equal to:

$$c_r = 2D\rho v_s\left(1+\frac{v_p}{v_s}\right) \quad (6)$$

Where $v_p$ and $v_s$ are related through the soil Poisson's ratio $\vartheta$when linear elastic material behavior is assumed:

$$v_p = v_s\sqrt{\frac{2(1-\vartheta)}{1-2\vartheta}} \quad (7)$$

Consequently, $v_p$ tends to infinity if Poisson's ratio approaches 0.5 (un-drained soil material behavior), which is not realistic. According to Gazetas and Dobry [11] $v_p$ maybe better estimated as:

$$v_p = \frac{3.4v_s}{\pi(1-\vartheta)} \approx 2v_s \quad (8)$$

Where they used Lysmer's [16] analog wave velocity, derived for surface foundations subjected to vertical oscillations. In their study, Gazetas and Dobry [12] also proposed an alternative expression that is based on assuming radiating waves in four quarter-planes (shear waves for two quarter-planes and compression waves for two quarter-planes) and assume a vertical plane-strain situation. Adding total energies that are radiated away will then yield the following expression for the dashpot coefficient:

$$c_r = 2D\rho_s v_s\left[1+\left(\frac{3.4}{\pi(1-\vartheta)}\right)\right]^{3/4}\left(\frac{\pi}{4}\right)a_0^{-1/4} \quad (9)$$

Where $a_0 = \pi fD/v_s$

In the design of spools, Equation3 will be used to introduce dashpots into the model. The radiation damping given by Equation 6 should be separated into two parts

$$C_r = 2D\rho V_s + 2D\rho V_p = 2D\rho V_s + 4D\rho V_s \quad (10)$$

In the axial and transverse direction, the dashpot constant is assumed to be

$$C_{rx} = C_{ry} = D\rho v_x \quad (11)$$

And for the vertical direction

$$C_{rz} = D\rho V_s\ . \quad (12)$$

Here, $D$ is the spool diameter. The effect of embedment, (which enhances damping (Gazetas 1991)), is ignored due to its uncertain nature as well as it is accounted for when determining the seabed friction coefficient. In the horizontal direction, the damping coefficient is half of Berger's equation [3], since in the analyses dashpot acts both in tension and compression, hence half. The reduction of radiation damping in the vertical direction by a factor of 4 is to acknowledge that the soil is a half-space (reduction by a factor 2) and spools tendency to lift (no damping in tension). Though the recommended values are half as much as researchers for which reported good fit between analysis and experiment (see El-Naggar and Bentley, [5]), and less than 1/8 of allowed by ASCE4-98, it is believed to be a good approximation to reflect the direction as the contact of spools with the seabed is not certain.

In this work damping related to the rotational degrees of freedom is neglected as per the Berger approach [3].

Most spools do not rest on the surface of the soil but are partly embedded. Embedment is known to increase both stiffness and damping of the foundation system, but the increase in damping is more significant (Novak, [26]). The effect of embedment on the soil damping will be ignored.

**Table 2 Average soil damping and average reduction factors (+- one standard deviation) for shear wave velocity$v_s$ and shear modulus $G$ within 20m depth (Table 4.1 of Euro Code 8 [8]).**

| Ground acceleraions ratio, α·S | Damping ratio | $\frac{V_S}{V_{S,\max}}$ | $\frac{G}{G_{\max}}$ |
|---|---|---|---|
| 0.10 | 0.03 | 0.90 (±0.07) | 0.80 (±0.10) |
| 0.20 | 0.06 | 0.70 (±0.15) | 0.50 (±0.20) |
| 0.30 | 0.10 | 0.60 (±0.15) | 0.36 (±0.20) |

Shear modulus and damping parameters must be measured by laboratory or field tests. Average reduction factors are given in Table 4.1 of Eurocode [8] and are reproduced in this study in Table 2. The peak ground acceptation, in conjunction with Table 2, will be used to determine the degradation of the shear modulus. It is suggested to ignore the soil hysteric damping in this design. However, if it is included, then no higher than 0.1 for the shear strain must be assumed;

i.e. the damping ratio should not exceed 10%, except by special studies.

## 8. Implementing Structural Damping

Non-linear time-domain analysis with direct time integration is used to address geometric or material nonlinearities in seismic analysis of the spool-soil system. One method of implementing material damping in a non-linear dynamic analysis is Rayleigh damping. Material damping for steel is specified in codes of practice as a percentage of critical damping. Since damping is not constant for all frequencies, assuming the same damping for all modes will over damp the system. Rayleigh damping approach allows calibrating its constant for two or more modes. A reasonable approach would be to enforce a Rayleigh damping curve that matches prescribed modal damping for the first and (say) tenth mode. There are other suggestions in the literature on how to calibrate the Rayleigh damping.

The damping of the structure is assumed to be viscous type and frequency dependant for the sake of convenience in the analysis. The proportional damping, or Rayleigh damping, also known as the classical damping expresses damping as a linear combination of the mass and stiffness matrices, that is,

$$C = \alpha M + \beta K \qquad (13)$$

Where$\alpha$ and$\beta$ are real scalars with 1/sec and sec units respectively. The real normal modes are preserved in classically damped systems. However, the accuracy of response may be questionable because this approach is formulated for the linear response of the structure which may not be the available situation for all cases (i.e. structures with nonlinearities).

## 8. Concluding Remark

This part of a three parts paper [36 and 37] summarises data needed for the design of rigid subsea spools and where the background information can be found. The aim is to provide the designers of the subsea spool enough background data for their work. In summarising research papers the focus was on the modeling of the rigid subsea spool with a reasonable computational cost. The question of spool installation tolerances, soil, and structural damping, are discussed in this part.

The second part [36] focus is on the requirements of ISO for the aseismic design of rigid spool. The third part deals with the design of rigid spools.

## 9. References


1. ASCE4-16, (2016), *Seismic Analysis of Safety-Related Nuclear Structures*. Published by ASCE to replace ASCE4-98 Seismic Analysis of Safety-Related Nuclear Structures and Commentary
2. Applied Technology Council (ATC) (1996), *Seismic Evaluation and Retrofit of Concrete Buildings ATC-40,* Volume 1 and 2 November.
3. Berger, B. S. (1977), *Vibrations of An Infinite Orthotropic Layered Cylindrical Viscoelastic Shell in An Acoustic Medium*, Mechanical Engineering, 99, 105.
4. Boulanger, R. W., Curras, C. J., Kutter, B. L., Wilson, D. W., & Abghari, A., (1999), *Seismic soil-pile-structure interaction experiments and analyses,* Journal of Geotechnical and Geoenvironmental Engineering*, 125,* 750-759.
5. El Naggar, M. H., and Bentley, K. J. (2000), *Dynamic analysis for laterally loaded piles and dynamic p-y curves,* Canadian Geotechnical Journal, 37, 1166-1183.
6. El Naggar, M. H. (1996), *Nonlinear analysis for dynamic lateral pile response*, Soil Dynamics and Earthquake Engineering, 15, 233-244.
7. *El Naggar, M., Shayanfar, M.A., Kimiaei, M., Aghakouchak, A.A.,*(2005), *Simplified BNWF model for nonlinear seismic response analysis of offshore piles with nonlinear input ground motion analysis,* Canadian Geotechnical Journal, 42, 2, pp. 365-380.
8. Eurocode 8: (2004) *Design of structures for earthquake resistance*.
9. Gazetas, G., (2012), *Nonlinear Soil-Foundation-Structure Interaction*, Proc.2nd International Conference on Performance-Based Design in Earthquake Geotechnical Engineering.
10. Gazetas, G. (1991), *Formulas and Charts for Impedances of Surface and Embedded Foundations*, Journal of Geotechnical Engineering 117, 1363-1381.
11. Gazetas, G. & Dobry, R. (1984a), *Horizontal Response of Piles in Layered Soils*. Journal of Geotechnical Engineering-ASCE*, 110,* 20-40.
12. Gazetas, G. & Dobry, R. (1984b), *Simple Radiation Damping Model for Piles and Footings,* Journal of Engineering Mechanics-ASCE, 110, 937-956.
13. Hardin, B. O., and Drnevich, V. P., (1972), *Shear Modulus and damping in soils*, Proc.ASCE: Journal of the Soil Mechanics and Foundations Division, 95(SM6), 1531-1537.
14. Ghannad, A.M., and Jahankha, (2004), *Strength Reduction Factors Considering Soil-Structure Interaction*, 13th World Conference on Earthquake Engineering Vancouver, B.C., Canada August 1-6, 2004 Paper No. 2331
15. Ghannad M.A., Fukuwa N. and Nishizaka R. (1998), *A Study on Frequency and Damping of Soil-structure Systems Using Simplified Model*, Journal of Structural Engineering (AIJ), 1998; 44B, 85-93.

16. Lysmer, J. and Kuhlmeyer R.L. (1969), *Finite Dynamic Model for Infinite Media*, Journal of Engineering and Mechanical Division, 859-877.
17. Jafarieh, A.H., and M. A. Ghannad M. A. (2014), *The Effect of Foundation Uplift on Elastic Response of Soil-Structure Systems*, International Journal of Civil Engineering, Vol. 12, No. 2, pp 244-256.
18. ISO 19902:2007, (2007), Petroleum and natural gas industries — Fixed steel offshore structures, Seismic Design Procedures, and Criteria.
19. ISO 19901-2, (2004), Petroleum and Natural Gas Industries – Specific Requirements for Offshore Structures – *Part 2: International Organization for Standardization: Seismic Design Procedures and Criteria.*
20. ISO 19901-4, (2002), Petroleum and Natural Gas Industries – Specific Requirements for Offshore Structures – *Part 4: International Organization for Standardization: Geotechnical and Foundation Design Considerations.*
21. Idriss, I. M., and Sun, J. I. (1992), *SHAKE91— A computer program for conducting equivalent linear seismic response analyses of horizontally layered soil deposits*, User manual, Univ. of California at Davis, Davis, Calif.
22. Ishibashi, I., and Zhang, X. J. (1993), *Unified dynamic shear moduli and damping ratios of sand and clay,* Soils Found., 33(1), 182–191.
23. Makris, N. & Gazetas, G. (1992), *Dynamic Pile Soil Pile Interaction- Lateral and Seismic Response*, Earthquake Engineering & Structural Dynamics, 21, 145-162.
24. Matlock, H., (1970), *Correlations for the design of laterally loaded piles in soft clay*, Preprints Second Annual Offshore Technology Conference, 1, 577-588.
25. Nogami, T., Otani, J., Konagai, K., & Chen, H. L., (1992), *Nonlinear Soil-Pile Interaction-Model for Dynamic Lateral Motion*, Journal of Geotechnical Engineering-ASCE, 118, 89-106.
26. Novak, M., (1974), *Dynamic stiffness and damping of piles*, Canadian Geotechnical Journal, 11, 574- 598
27. Seed, H. B., and Idriss, I. M. (1970), *Soil moduli and damping factors for dynamic response analysis*, *Rep. No. EERC 70-10*, Earthquake Engineering Research Center, Berkeley, Calif.
28. Seed, H. B., Wong, R. T., Idriss, I. M., and Tokimatsu, K., (1986), *Moduli and damping factors for dynamic analysis of cohesionless soils*, *J. Geotech. Eng.*, 112~111, 1016–1032.
29. Spears, R.E. and S. R. Jensen (2009), *Approach for Selection of Rayleigh Damping Parameters Used for Time History Analysis*, 2009 ASME Pressure Vessel and Piping Division Conference, PVP2009-77257, Prague
30. Stokoe, K. H., II, Darendeli, M. B., Andrus, R. D., and Brown, L. T. (1999), *Dynamic soil properties: Laboratory, field, and correlation studies,* Proc., 2nd Int. Conf. on Earthquake Geotechnical Engineering, Vol. 3, Lisbon, Portugal, 811–845.
31. Darendeli, M. B., and Lee, N. J. (1995), *Correlation study of nonlinear dynamic soils properties,* Final Rep. to Westinghouse Savannah River Company,
32. Vesic, M., (1961), *Beam on the elastic subgrade and the Winkler hypothesis,* Proc. International Conference Soil Mechanics and Foundation Engineering, Paris*, 1,* 845-850.
33. Vucetic, M. and Dobry, R., (1991*), Effect of Soil Plasticity on Cyclic Response,* Journal of Geotechnical Engineering-ASCE, 117, 89-107.
34. Wolf J.P., (1994), *Foundation vibration analysis using simple physical models*, Prentice-Hall Englewood Cliffs, N.J. The USA.
35. Wolf, J. P. & Deeks, A. J. (2004), *Foundation Vibration Analysis: A Strength-of-Materials Approach*. Elsevier, Oxford, U.K.
36. Yasseri, S, (2020), *Seismic Design of Subsea Spools per ISO: Part II- Seismic requirements*, IJCOE, Vol.4, No.2 , Summer 2020.
37. Yasseri, S., (2020), *Seismic Design of Subsea Spools per ISO: Part III- Analysis & Design*, IJCOE

**Table of abbreviations**

| Abbreviation/ Acronym | Description |
|---|---|
| CDT | Cool Down Time |
| CPT | Cone Penetrometer Test |
| CRA | Corrosion Resistant Alloy |
| CMS | Corrosion Monitoring Spool |
| DEH | Direct Electrical Heating |
| ECA | Engineering Critically Assessment |
| FE | Finite Elements |
| FTA | Flowline Termination Assembly |
| ID | Inside Diameter |
| LB | Lower Bound |
| MEG | Mono Ethylene Glycol |
| MCM | Manifold Control Module |
| OD | Outside Diameter |
| PMA | Production Manifold Assembly |
| SIWHP | Shut-in Well-head Pressure |
| SMLS | Seamless |
| UB | Upper Bound |